Materials Transactions, JIM, Vol. 41, No. 4 (2000) pp. 492 to 498

Oxidation of Metallic Binder Powder and its Influence on Mechanical Properties Metal-Diamond Composite

V. Jokanović[1], P. Živanović[2], R. Ćurčić[1], G. Djurković[1] and D. Izvonar[3]

[1]*Institute for Technology of Nuclear and Other Mineral Raw Materials, Franchet D' Eperey 86,11000, Belgrade, Yugoslavia*
E-mail: bjelun@ptt.yu
[2]*Institute of Technical Sciences of the Serbian Academy of Sciences and Arts, 11000, Belgrade, Yugoslavia*
E-mail: zhile@itn.sanu.ac.yu
[3]*High Technical School, Arandjelovac, Yugoslavia*

In this paper, the properties of metallic binders based on Co, Fe, bronze and their influence on mechanical characteristics of metallic binder-diamond composites, obtained by hot pressing of these powders, were analyzed. At the same time, the influence of the metallic powder aging process on the mechanical characteristics of metallic binder compacts and corrosion of diamond grain, conditioned by the oxygen bonded to metallic powder particles, were separately considered.

(Received February 16, 1999; In Final Form February 4, 2000)

Keywords: *aging, metallic binder, oxidation, diamond grain, hardness, toughness, oxide layer, relative humidity, bound oxygen, pits etching, composites*

1. Introduction

The diamond tools with metallic binders are used for processing of aluminium, copper, zinc and manganese-based alloys, very hard alloys based on wolfram, ceramics, glass, semiconducting materials, cermets, refractory bricks, concrete, stone, wood, plastics, reinforced plastics, caoutchouc, *etc.*

Depending on the type and shape of the product, the starting powder should satisfy different requirements: physical (size distribution, particle shape and surface condition), chemical (contents of the basic metal and ingredients, inclusion of gases in chemically bonded, adsorbed or dissolved states), and technological (bulk mass, yielding, compressibility) requirements. In powder metallurgy, when producing the diamond tools, the most often used metallic binders are Co powders and their alloys, either alone or in combination with other metallic powders, such as Cu, Sn, Fe, Ni, Zn, Mn, Mo, Bi, Ag, W, Ti, V, and copper based alloys: Cu–Al, Cu–Sn, Cu–Fe–Sn–Ni, Cu–Sn–Ti, Cu–Al–Zn, Cu–Ag, Cu–Cr–Zr, Cu–Zr, Cu–Cd, Cu–Ag, Cu–Ti, Cu–Ga–Cr, Cu–Ga–Ti.[1–3)]

For sintering of metallic binder-diamond composite hot pressing was employed because it is economical and enables control of the compact properties via control of their microstructure.[4–9)] One of the factors that restrict use of the given powder for synthesis of metallic binder-diamond compacts is oxidation of the powder particles occurring during powder synthesis and particularly during powder aging prior to its use. Therefore, in this and a number of the previous works[10–14)] dealing with different aspects of this phenomena, influence of the parameters such as relative air humidity, temperature and aging time on process of metal powder oxidation was investigated. Beside that, for more precise defining of the consequences of powder oxidation during its aging, influence of the powder oxidation parameters on mechanical properties of hot pressed metallic binder-diamond compacts and diamond grain corrosion process occurring during hot pressing of these compacts were paid particular attention.

2. Experimental

For synthesis of metallic binder-diamond compacts, commercial mixtures of metal powders-cobalt, iron and bronze powders, denoted by B_1, B_2 and B_3, were used. The B_1 and B_2 powders denote cobalt powders, while B_3 denotes the mixture of Co, Fe and bronze powders.[10–14)] Characterization of powders was carried out by a method of the emission spectrophotometry, identifying all contained impurities (on ingredient level, or in traces). The quantitative analysis of ingredients present in B_1, B_2 and B_3 powders was performed by a method of the atomic absorption spectrometry, using "Perkin-Elmer 703" device (accuracy 1 ppm). The alkalis were determined by the flame emission spectrometry (accuracy 10 ppm), using "Dr Lange" device. For more precise determination of the alkalis content, teflon containers were used instead of the glass ones. The content of oxygen was determined by coulometric method of oxygen extraction by inert gas (the method by Abresch Lemm). The base was analyzed by usual analytical methods (Sn-gravimetrically, Fe-volumetrically, Cu and Co-electrochemically).

The size distribution and morphology of particles were determined by the analysis of the images, obtained by scanning electron microscopy using Jeol JSM 5300 device, at the voltage of 25 kV and the current density of 17 μA. The hardness was determined by the Brinell method using Alpha Sweden equipment (conditions: ball diameter 5 mm, load 750 kp and time 15 s). The toughness was determined by Charpy method using Alfred Amsler Sch. Equipment.

Because of it's high inclination to agglomeration, cobalt powder was prepared by dispersion in suspension of the amyl-

acetate solution in collodion, and subsequently placed and fixed on the surface of the brass support. For better contrasting, the powder was evaporated by graphite and shadowed by gold in the ionic evaporation device ($p \sim 1.3 \times 10^2$ Pa, $t = 30$ min). The presence of impurities was analyzed by a method of the point scanning, using EDS analyzer GX-2000 S (Oxford Instruments QX-2000 S), in the X-ray range of 0.5–20 kV, connected to the scanning electron microscope.

In order to investigate the influence of the aging conditions on the amount of bound oxygen, and thus on the mechanical and oxidational characteristics of the metallic powder-diamond composites, the powders were exposed to the aging process under different conditions of temperature, T, relative humidity, φ and aging time, t, as follows: $T = 20°C$, $\varphi = 55\%$, 75% and 100%, $t = 2$, 6, 18, 24, 90 and 128 h (series 1, 2 and 3 respectively); $T = 19$–$24°C$, $\varphi = 50$–55% and $t = 24$ days (series 4); $T = 30°C$, $\varphi = 100\%$ and $t = 128$ h (series 5).

All samples (B_1, B_2 and B_3) exposed to aging were hot pressed at the temperatures of 600–800°C (depending on the type of powder) and at a pressure of 35 MPa, for 5 min. After that, hardness (*HB*) and toughness by Sharpy (*CVN*) of all samples were determined. Besides, metallic binder-diamond compacts were examined as to the diamond grain corrosion, by analyzing image of their surface taken after hot pressing was completed.

3. Results and Discussion

3.1 Characterization of powder

Characterization of the starting powder mixtures composed of B_1, B_2 and B_3 powders, was performed by different chemical analyses and analyses of the images obtained by scanning electron microscopy (Table 1, Figs. 1–5). On the basis of so obtained results, influence of the purity of the starting powders, systems (B_1, B_2, B_3) and their dispersions on mechanical and oxidational characteristics of compacts obtained by hot pressing of these powders and their mixtures with diamond powder were investigated.

From the aspect of influence of the chemical composition on the properties of the hot pressed compacts, the content of oxygen bound to metallic powder particles were regarded as main factor. For the comparison of the influence of the bound oxygen on oxidation degree of B_1, B_2 and B_3 powders, the amount of oxygen bound to the average sized powder particle was selected as an optimal criterion. In the case of a complex B_3 powder, each individual constituent (Co, Fe, bronze) and the powder as a whole (B_3) were assessed.

Chemical and microscopical analyses showed that B_1 and B_2 powders contain only Co particles whose average sizes were 0.8 μm (B_1) and 2 μm (B_2), and maximal sizes of 1 μm (B_1) and 2.5 μm (B_2), respectively. B_3 powder is composed of Co, Fe and bronze powders, whose average sizes were 2, 12 and 80 μm, respectively. The average particle size of B_3 powder mixture was 37.80 μm. The cobalt particles were spherical to rod-like (Figs. 1, 2), the Fe particles spherical to egg-like, of smooth surface. Different from the Fe-particles,

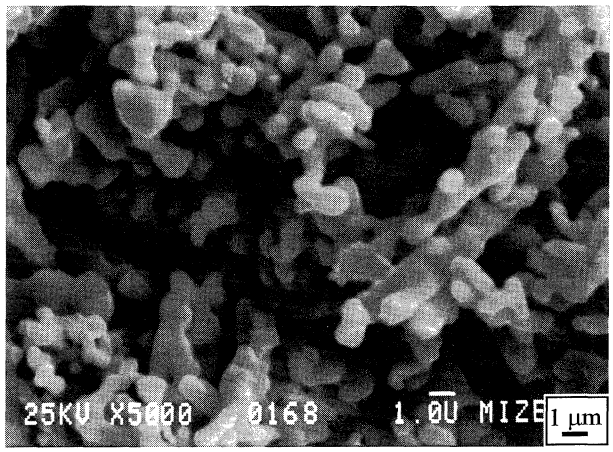

Fig. 1 SEM micrograph of the cobalt particles in B_1 binder.

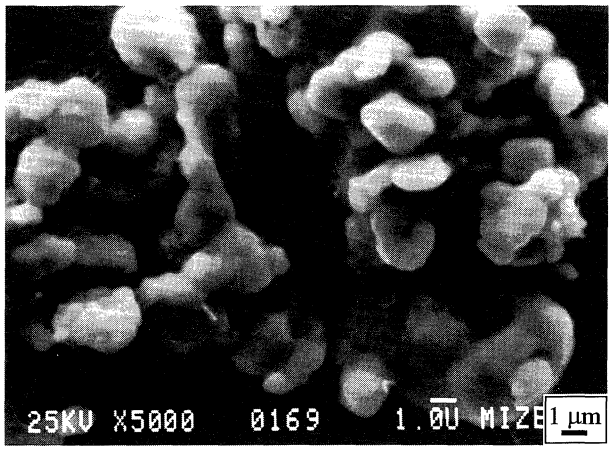

Fig. 2 SEM micrograph of the cobalt particles in B_2 binder.

Fig. 3 SEM micrograph of the bronze and cobalt particles in B_3 binder.

Table 1 Chemical compositions of the binding powders.

Binder	Elements				(mass%)
	Co	Cu	Sn	Fe	O
B_1	99.2	0.04	—	0.015	0.705
B_2	99.4	0.11	—	0.145	0.326
B_3	13.8	60.1	10.5	14.90	0.258

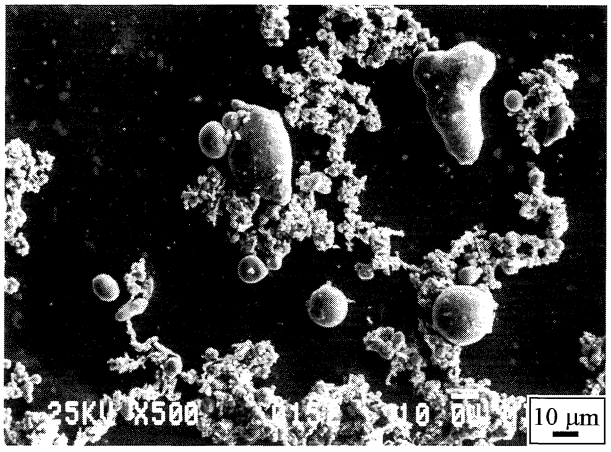

Fig. 4 SEM micrograph of the iron particles in B_3 binder.

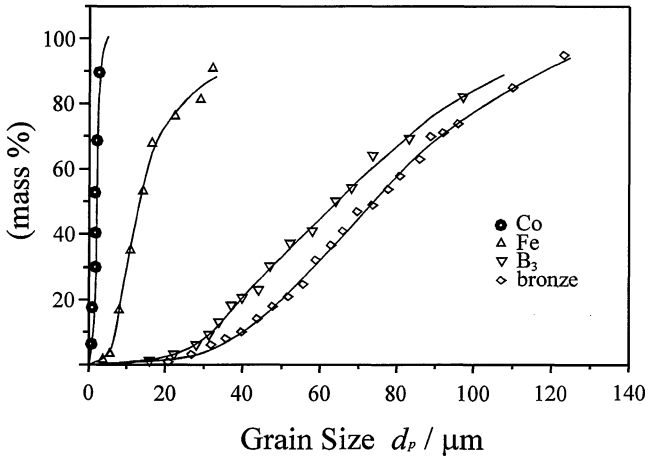

Fig. 5 Particle size distribution for B_3 binder components and binder as a whole.

bronze particles were of irregular shape and rough surface.

Since the average particle size was chosen for the comparison of oxidation degree of different powders, beside total amount of oxygen bound per unit mass (T_1) of powders, the amount of oxygen bound to a particle of a defined size and the amount bound to the unit surface of such particle were also determined. Calculated amounts of oxygen bound to the average sized particle were: 1.6×10^{-14} g for Co (B_1), 11.9×10^{-14} g for Co (B_1 and B_2) and 5.6×10^{-10} g for Fe (B_3).

The amounts of oxygen bound per a unit surface were: 1.1×10^{-2} g/m^2 for Co (B_1), 9.4×10^{-3} g/m^2 for Co (B_1 and B_2) and 30.9×10^{-2} g/m^2 for Fe (B_3). As evident from the obtained data, the amount of oxygen bound to the unit surface was the highest for the Fe-powder, whose chemical activity was the highest.

For better understanding of the influence of bound oxygen on surface oxidation of metallic powders, thickness of oxide layer formed during oxidation was calculated according to the following expression (see Appendix):

$$D_r = r_p - \left(r_p^3 - \frac{3m_r}{4\rho\pi}\right)^{1/3} \quad (1)$$

where: D_r is thickness of oxide layer formed on average sized particle,
r_p is radius of the particle,
m_r is the mass of the oxide layer,
ρ is density of materials that the particle is made of (Co, Fe and bronze)

The thickness of oxide layers were 2 nm for Co particle (B_1), 3 nm for Co particles (B_2 and B_3) and 18 nm for Fe particle (B_3).

3.2 Powder aging

In order to define the influence of the oxidation conditions (temperature, T, relative air humidity, φ, time, t), all the metallic powders (B_1, B_2 and B_3) were exposed to oxidation under controlled conditions, as can be seen in Table 2. As evident from Table 2, duration of oxidation (2–128 h) at a given air humidity (55%) and temperature (20°C) was least influential. The differences between 0.12% (B_1), 0.02% (B_2) and 0.05% (B_3) are clearly seen. As opposed to the influence of time, the influence of temperature on oxidation of metallic powder was obviously stronger, as can be seen from the data contained in the same table (0.31% for B_2, 0.34% for B_1 and 0.13% for B_3 sample, at the relative humidity $\varphi = 100\%$ and exposure time) $t = 128$ h. According to Table 2, the main factor of oxidation was relative air humidity. If the relative air humidity changed from 55 to 100%, at 20°C, the amount of bound oxygen increased by 2.67% for B_1 powder, 2.04% for B_2 powder and 1.26% for B_3 powder. For this reason, the amount of bound oxygen (in comparison to the total weight of metallic powder) for the Co powders (B_1, B_2 and B_3) depending on relative air humidity was investigated separately (Fig. 6).

By fitting experimental data for Co powders in B_1, B_2 and B_3 mixtures, it was found that Boltzman sigmoidal functions is most appropriate to describe dependency between the amount of bound oxygen and air humidity. This function can be written in the following form:

Table 2 Change in oxygen content depending on the aging conditions, mass%.

Experimental series	Aging conditions	Binder		
		B_1	B_2	B_3
1	$T = 20$°C $\varphi = 55\%$ $t = 2$–128 h	0.96–0.98	0.35–0.48	0.28–0.33
2	$T = 20$°C $\varphi = 75\%$ $t = 128$ h	2.71	2.02	0.86
3	$T = 20$°C $\varphi = 100\%$ $t = 128$ h	3.65	2.52	1.59
4	$T = 19$–24°C $\varphi = 50$–55% $t = 24$ days	0.79–1.13	0.37–0.76	0.31–0.62
5	$T = 30$°C $\varphi = 100\%$ $t = 128$ h	3.98	2.83	1.72

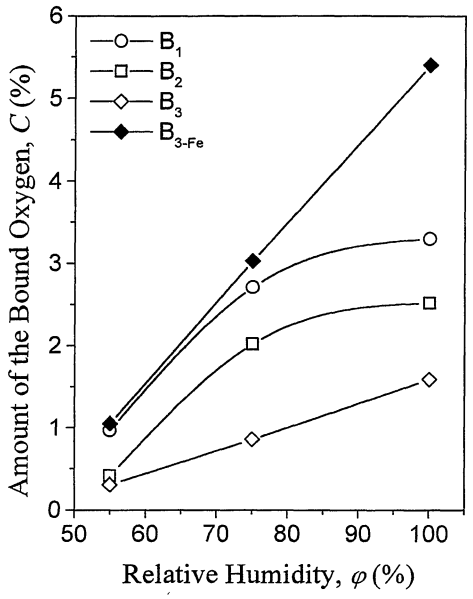

Fig. 6 Concentration of bound oxygen depending on the relative humidity for cobalt and iron powders.

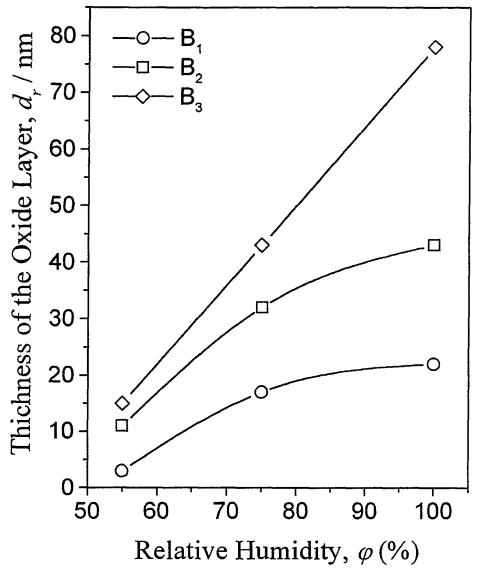

Fig. 7 Thickness of the oxygen layer on metal powder particles depending on relative air humidity for cobalt and iron powders.

$$C = \frac{A_1 - A_2}{1 + e^{(\varphi - \varphi_0)/\Delta\varphi}} + A_2 \qquad (2)$$

where: C is the amount of bound oxygen,
φ is air humidity,
A_1, A_2, φ_0 and $\Delta\varphi$ are adjustment constants.

The given function was obtained by fitting the data presented in Table 2 using the Origin 5.0 Standard. The values of the adjustment constants (determined by iterative method) for Co powder (B_1), were: $A_1 = 2.374$; $A_2 = 3.373$; $\varphi_0 = 50.99$ and $\Delta\varphi = 12.42$; for Co powder (B_2 and B_3), $A_1' = 3.20$, $A_2' = 2.27$, $\varphi_0' = 50.19$ and $\Delta\varphi' = 8.35$. For Fe powder (B_3), the amount of bound oxygen depending on relative air humidity was fitted by a linear function of the following type:

$$C = A'' + B\varphi \qquad (3)$$

where: A'' and B are the adjustment constants having the values: $A'' = -4.39$ and $B = 0.10$ and for B_3 powder as the whole $A'' = -1.27$ and $B = 0.03$.

Analogous to the dependency shown in Fig. 6, dependence of the thickness of the oxide layer formed on the surface of metallic powder particles on air humidity and the amount of bound oxygen (Figs. 7 and 8) were analyzed. By using computer program a type of function appropriate to given experimental data was determined. For Co powders (B_1, B_2 and B_3), the diagram presented in Fig. 7 is best described by Boltzman sigmoidal function, with the thickness of oxide layer (oxidation ring), d_r, on the surface of metallic particle taken as independent variable for eq. (2), instead of the amount of bound oxygen. The adjustment constants (determined by iterative method) in equation $d_r = f(\varphi)$ for Co powder (B_1) were: $A_1^{III} = -3.44$; $A_2^{II} = 22.45$; $\varphi_0^{II} = 63.69$ and $\nabla\varphi^{II} = 9.81$ and for Co powders (B_2 and B_3), these were: $A_1^{III} = -22.37$; $A_2 = 46.59$; $\varphi_0^{III} = 55.90$ and $\Delta\varphi^{III} = 15.17$.

By fitting experimental data relating to the thickness of the oxide layer on Fe powder depending on air humidity, it was found out that the most appropriate analytical form to describe such function is linear function, which can be written in the following form:

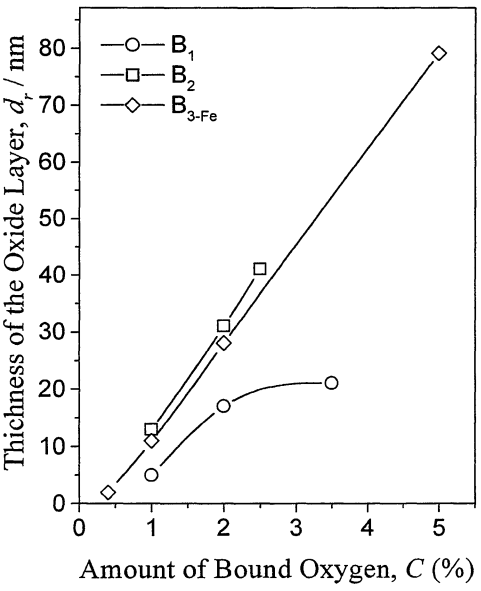

Fig. 8 Thickness of the oxygen ring on the metal powder particles depending on amount oxygen bound to cobalt and iron powders.

$$d_r = d_{r0} + B_r\varphi \qquad (4)$$

where: d_r is thickness of oxide layer,
φ is relative air humidity, and
d_{r0} and B_r are adjustment constants.

These constants, obtained by iterative method for the given case, have the following values: $d_{r0} = -62.0$; $B_3 = 1.4$.

In a similar way, it was shown that the diagrams in Fig. 8 for Co powder are best described by Boltzman sigmoidal function, $d_r = f(C)$, while Co powders (B_2 and B_3) and Fe powder (B_3) are best described by linear function $d_r = f(C)$

(modified eqs. (2) and (3)).

Adjustment constants (iterative method) in Boltzman function, for Co (B_1) were as follows: $A_1^{VI} = 21.79$; $A_2^{IV} = 22.22$; $C_0 = 0.67$ and $\Delta C_0 = 0.61$; for Co powder (B_2 and B_3), these constants were: $A^{VII} = -5.16$ and $B^{I} = 18.18$; for Fe (B_3) powder, these were: $A^{VIII} = -5.36$ and $B^{II} = 16.84$.

When analyzing the diagrams presented in the Figs. 6 and 7, it can be seen that the amount of bound oxygen (Fig. 6) and, analogue to that, the thickness of oxide layer on the surface of the Co particles (Fig. 7) linearly increases with increase of relative air humidity from 55 to 75% for all Co powders. With further increase of air humidity from 75 to 100%, an increase in amount of bound oxygen (Fig. 6) and in thickness of oxide layer slow down (Fig. 7), in accordance with the given Boltzman sigmoidal functions. Different from Co powders, linear increase of bound oxygen and thickness of oxide layer on the surface was registered for B_3 (Fe powder) in the whole range of relative air humidity, from 55 to 100% (Fig. 6) and (Fig. 7). While a slowed increase of oxide layer on Co powder particle with increase of air humidity above 75% can be explained by slowed diffusion through the already formed oxide layer, which is in agreement with theoretical expectations, further intense increase of thickness of the oxide layer formed on Fe particles (B_3 powder) is somewhat more complex. Here, two factors are particularly important: the surface activity of Fe powder and the rate of oxygen transportation from the surface towards the interior of the particle. Kinetics at which the energy centers on the powder particle surface are occupied by the oxygen molecules (molecules of adsorbed water) would depend on the first factor, while the migration of oxygen from the surface and liberation of places on the surface of powder particles for adsorption of the fresh amount of oxygen would depend on the second factor.

3.3 Influence of powder aging on mechanical properties of hot pressed compacts

The influence of oxidation parameters on mechanical properties of compacts obtained by hot pressing of metallic powders (hardness *HB*, and toughness *CVN*) was analyzed under various conditions of oxidation, for all metallic powders (B_1, B_2 and B_3).

The data given in Table 2 show that process of oxidation is most strongly influenced by relative air humidity because it has decisive influence on amount of oxygen bound by the powder particle. For this reason, its influence on previously mentioned mechanical properties (hardness and toughness) of hot pressed composite compacts was analyzed separately (Fig. 9). Contrary to expectations, although influence of oxidation on certain properties, for instance toughness is beyond doubt (as will be analyzed in the forthcoming text), it is quite obvious that oxidation has not significant influence on hardness which is confirmed by the fact that their values are of the same order of magnitude for each value of relative humidity. In all the powders (B_1, B_2 and B_3), change of hardness by changing relative air humidity from 55% to 100% was almost negligible. Only in the case of B_2 powder, some notable change of toughness was registered; it can be described by Boltzman sigmoidal function (the given function was obtained by fitting the data presented in Table 2 using the Origin

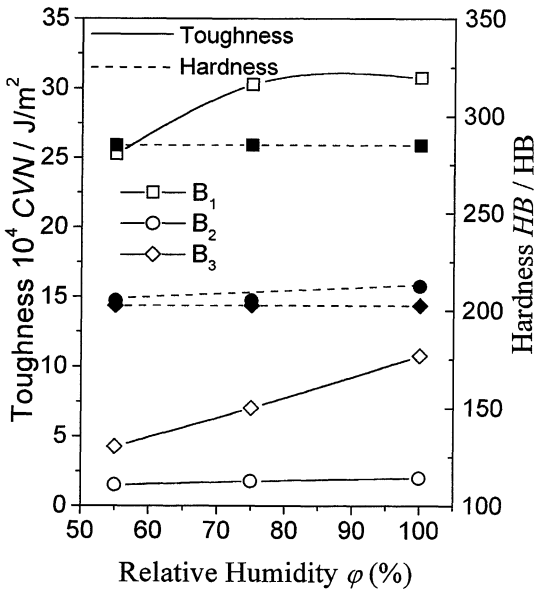

Fig. 9 Hardness and toughness of hot pressed metallic binder compacts depending on relative air humidity.

5.0 Standard):

$$CVN = \frac{A_1^{VIII} - A_2^{IV}}{1 + e^{(\varphi - \varphi_0)/\Delta\varphi^{IV})}} + A_2^{IV} \qquad (5)$$

where *CVN* is toughness of compact, and φ is relative air humidity. By a method of iteration the values of the adjustments constants were determined: $A_1^{VII} = 24.12$; $A_1^{IV} = 30.96$; $\varphi_0^{V} = 63.17$ and $\Delta\varphi^{IV} = 5.04$. In the case of B_3 powder, dependency of toughness on relative air humidity (Fig. 9) was linear:

$$(CVN = A^{VIII} + B_{\varphi}^{III}). \qquad (6)$$

Adjustment constants have the values: $A^{VIII} = 2.80$ and $B^{III} = 0.13$. An increase of the compact toughness (Fig. 9, curves 2 and 3; powders B_2 and B_3) with increase of relative air humidity is probably the consequence of the powder particle structure, comprising metal core and oxide ring by oxidation occurring in the course of the powder synthesis and powder aging. Therefore, an explanation for toughness increase with increase of relative air humidity and consequent higher degree of oxidation in the given system can be searched for in a specific structure even after hot pressing, with clearly defined boundary between the phases of metal and oxide, thus enabling changing of path direction and/or branching of the crack under appropriate load.

3.4 Corrosion of the diamond grain

In Figs. 10(a) and (b), the morphology of corroded diamond grains during hot pressing of metallic binder (B_3)-diamond composite is presented.

It is evident from the layout of the diamond surface that corrosion of grains is particularly intense in the places such as corners, as well as other parts of the diamond grain with greater surface defects. These high-energy centers of the diamond grain surface were exposed to the activity of oxygen bound on the surface of metallic powder during hot pressing.

Table 3 Mechanical properties of the metallic binders after hot pressing.

Experim. series	Aging conditions	Binder					
		Hardness, B			Toughness·10^4 (J/m^2)		
		B_1	B_2	B_3	B_1	B_2	B_3
1	$T = 20°C$ $\varphi = 55\%$ $t = 2$–128 h	189–221	285	205	1.3–1.6	23.9–27.4	4.5–4.08
2	$T = 20°C$ $\varphi = 75\%$ $t = 128$ h	198–221	286	205	1.8	31.3	7.3
3	$T = 20°C$ $\varphi = 100\%$ $t = 128$ h	200–255	285	208	2.0	34.2	10.5
4	$T = 19$–$24°C$ $\varphi = 50$–55% $t = 24$ days	187–232	285	210	1.2–1.6	26.3–29.5	4.7–5.9
5	$T = 30°C$ $\varphi = 100\%$ $t = 128$ h	239	285	209	2.1	35.3	11.2

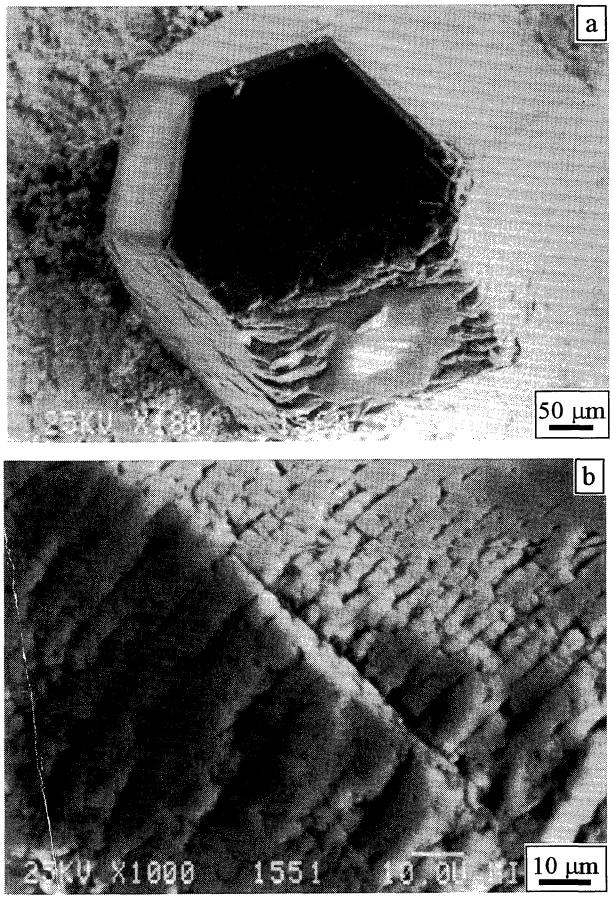

Fig. 10 . SEM micrograph of corroded diamond grain.

The mechanism of the grain corrosion itself involves decomposition and reduction of metal oxides present on the surface of metallic powder particles, followed by a reaction between free oxygen and carbon positioned in the centers of the highest energy (centers of defects concentration). In the places of intense reaction, deep etching pits (holes) are formed, around which the rings or large surfaces or very deep damages of irregular shape, rounded corners *etc.*, are formed. In other places, this process is more moderate, forming a line of connected bands with certain "islands" or different surfaces and emphasized groove along the grain.

It should also be pointed out that occluded gases and products of reaction between carbon from diamond grain and oxygen are collected in rough spots and holes during sintering. This contributes to weakening of bonds between diamond grains and metal matrix. Under conditions of intense wearing, it facilitates drop out of the diamond grains from the metal matrix and shortens lifetime of the tools made out of such compacts.

4. Conclusion

In this paper, influence of the aging conditions (temperature, relative air humidity and time) on the amount of oxygen bound to cobalt powders of varying dispersity and a mixture of cobalt, iron and bronze powders were investigated.

Based on the present investigations, the following conclusions were derived:

— Total content of bound oxygen was maximal for the cobalt powder and minimal for the powder mixture composed of Co, Fe and bronze;
— Relative content of oxygen, the amount of oxygen bound to the unit surface was maximal for the mixed powder, due to exceptionally high activity Fe powder;
— Relative air humidity is the most significant parameter of the metallic powder activity;
— Time is the least influential parameter of metallic powder activity;
— The thickness of oxide layer formed on the surface of the powder particle depending on relative air humidity is fitted by Boltzman sigmoidal function for Co powders,

showing intense growth of formed layer for the humidity of 55–75%, followed by a slow growth at 75–100%; in the case of Fe powder, at 75–100%; this growth of thickness continues without interruption, which can be described by fitted exponential function;

— Mechanical properties (toughness and hardness) of hot pressed metallic binder-diamond compacts do not show some significant dependence on the amount of bound oxygen;

— Corrosion of diamond grains is in direct relationship with the amount of oxygen bound to metallic powder particles, *i.e.* with conditions of aging, particularly relative air humidity.

Appendix

The thickness of the oxide layer was calculated for the average size particle since this particle is regarded representative for size distribution of the whole system. In accordance with that, a mass of the oxide layer on the average size particle, m_p, can be expressed in the following way:

$$m_p = \frac{4}{3} r_p^3 \pi \rho - \frac{4}{3} r_c^3 \pi \rho, \tag{A·1}$$

where r_c is radius of the particle core, r_p is radius of the whole particle and ρ is the particle density.

If the thickness of the oxide ring is denoted D_r, it follows that:

$$D_r = r_p - r_c. \tag{A·2}$$

By replacing r_c with r_p-D_r in eq. (1) and its mathematical ordering, we finally obtain the following equation:

$$D_r = r_p - \sqrt[3]{r_p - \frac{3m_p}{4\pi\rho}}. \tag{A·3}$$

It is possible to express m_p as a summ of masses of the metal powder particle and oxygen bound to that surface, as it follows:

$$m_p = m_m + m_o, \tag{A·4}$$

where m_m is mass of metal and m_o is mass of oxygen bound to that particle.

On assumption that the following reaction takes place:

$$xM + yO = M_x O_y, \tag{A·5}$$

where x and y are respective numbers of metal and oxygen atoms, it follows that:

$$m_m = \frac{x}{y} \frac{A_m}{A_o} m_o, \tag{A·6}$$

where A_m and A_o are respective atomic masses of metal and oxygen.

Consequently, the ring mass can be expressed in the following way:

$$m_p = m_m + m_o = m_o \left(1 + \frac{xA_m}{yA_o}\right). \tag{A·7}$$

REFERENCES

1) I. Najdič and V. V. Turhal: *Isledovanije pročnosti sceplenija vanadijevih pokritij s almazom*, In-t sverhtverdih materialov AN USSR, Kiev, (1983), pp. 84–86.
2) F. V. Krasnickaja and M. Samohina: *Vzamodejstvije pripoev s disperrsnov pročečnoj medju pripajke*, In-t problemi materialovedenija AN USSR, Kiev, In-t Giprocvetmetalloobrabotka, Moskva, (1983), pp. 103–108.
3) I. Yu. Najdič and P. V. Umanskij: Sverhtverdie materiali, **16** (1982), pp. 26–29.
4) A. A. Šuljženko and B. I. Ginzburg: Sverhtverdie materiali, **46** (1987), pp. 23–28.
5) G. V. Gargin: Sverhtverdi materiali, **13** (1981), 9–11.
6) E. S. Simkin and N. V. Cipin: Sverhtverdie materiali, **56** (1989), pp. 29–33.
7) A. Yu. Gratsianov and N. B. Putinstev: *Metallicheskie poroshky iz rasplavov*, Metallurgija, Moskva, (1970), pp. 132–136.
8) L. Shonrong: Trans. Nonferrous Metals Soc., **3** (1993), 51–57.
9) M. G. Losshale and L. J. Alexandrova: *8th Int. Conf. Fracture*, Kiev, In-t sverhtverdih materialov Kiev, (1993), pp. 84–88.
10) V. Jokanović and S. Tomašević: *MAT TECH 90', The First Europian West-East Symposium on Materials and Processes*, Helsinki, European powder metallurgy association, (1990), pp. 239–248.
11) V. Jokanović, R. Ćurčić and D. Stanković: *4 International Metallurgical Symposium Metal 95*, Ostrava, Czech Society for New Materials and Technologies, (1995), pp. 143–149.
12) V. Jokanović, R. Ćurčić and G. Djurković: *International Conference on Powder Metallurgy and Particulate Materials*, Las Vegas, Metal Powder Industries Federation-APMI International, (1998), pp. 171–174.
13) V. Jokanović, R. Ćurčić, G. Djurković and P. Živanović: J. Mining and Metallurgy, **34** (1998), 139–152.
14) V. Jokanović, R. Ćurčić, G. Djurković, P. Živanović and D. Uskoković: *Powder Metallurgy World Congress*, Granada, European powder metallurgy association, **4** (1998), 229–233.